# VII. CATALYST SYNTHESIS AND CHARACTERIZATION METHODS

## VII.1. Catalyst Preparation and Physical Characterization

### Catalyst Synthesis Procedure

Precipitated iron catalysts were prepared using certified A.C.S. grade $Fe(NO_3)_2 \cdot 9H_2O$, $KHCO_3$, and $Cu(NO_3)_2 \cdot 2.5H_2O$. Silica and alumina supports were prepared from C.P. potassium silicate and aluminum sec-butoxide, respectively. Unpromoted and copper-promoted iron catalysts were prepared by a continuous co-precipitation method. An aqueous solution containing $Fe(NO_3)_3$ (0.6 M) and the required concentration of $Cu(NO_3)_2$, corresponding to the desired Fe/Cu ratio in the final catalyst, and a second solution containing aqueous $NH_3$ (2.7 M) were maintained in stirred glass vessels at 83 ± 3°C. The two solutions were separately conveyed by fluid pumps to a stirred vertical tubular reaction vessel that was maintained at 82 ± 1°C. Precipitation (to form $FeOOH/Fe_2O_3$ and $Cu(OH)_2$) occurred continuously as the two solutions were pumped upward through the vessel, while an in-line pH electrode was used to continuously monitor the pH of the reactor effluent. The flow rate of the $NH_3$ solution was normally fixed at 60 ml/min, while that of the $Fe^{3+}/Cu^{2+}$ solution was adjusted (typically to 90 ml/min) to give a precipitation pH value of 6.0 ± 0.2. As shown in Figure VII-1, if the reaction pH exceeded 6.2, precipitation of copper was incomplete, due to formation of the soluble $Cu(NH_3)_4{}^{2+}$ complex.

Collection of the slurried precipitate was made in ice-cooled vessels and was continued until one of the two solutions was consumed. The precipitate was then thoroughly washed by vacuum filtration to remove excess $NH_3$ and $NO_3^-$, using 10 liters of deionized, distilled water per 100 g (dry weight) of final catalyst. If the catalyst contained no $SiO_2$ or $Al_2O_3$ support/binder, the washed precipitate was dried in a vacuum oven for 48 h at 50°C to remove most of the excess water, and then for an additional 12 to 24 h at 120°C. Potassium promoter was added by impregnation of the dried Fe/Cu precipitate with a $KHCO_3$ solution of appropriate concentration. The final product was dried further in a vacuum oven for 16 h at 120°C.

Silica-supported catalysts were prepared by a modification of the above method. Impregnation with $SiO_2$ binder/support was accomplished by re-slurrying a 100 g aliquot (dry weight basis) of moist, undried precipitate in water, followed by addition of an appropriate amount of a dilute $K_2SiO_3$ solution containing 26.4 wt% $SiO_2$. Solution pH after $K_2SiO_3$ addition was 8 to 9, depending upon the amount of added silicate, and was adjusted to 6.5 by addition of aqueous $HNO_3$. The final pH adjustment was necessary both to ensure complete decomposition of

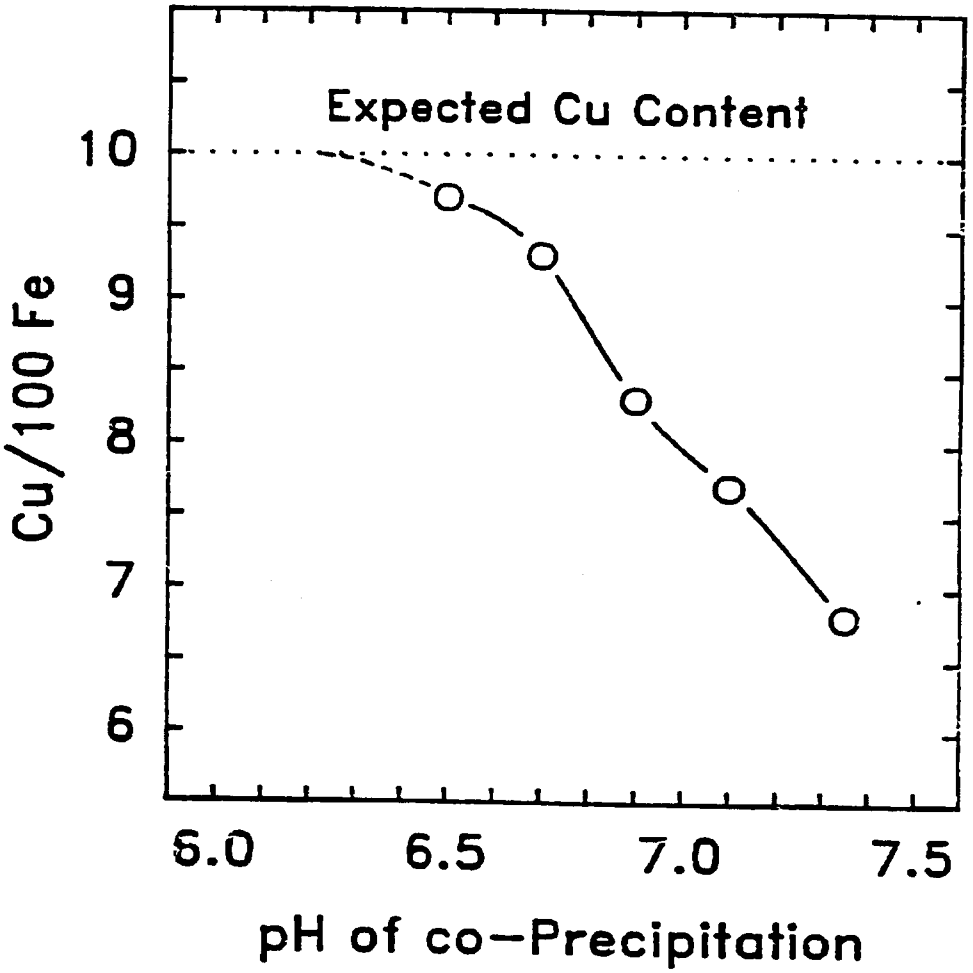

Figure VII-1 Effect of reaction pH on copper content of precipitated iron catalysts at 80°C

$K_2SiO_3$ (with its accompanying deposition of $SiO_2$) onto the $FeOOH/Fe_2O_3/Cu(OH)_2$ precipitate and to prevent loss of copper and/or iron by dissolution. The resulting silica-containing slurry was stirred at ambient temperature for 4 h to ensure complete penetration of the $K_2SiO_3$ solution into the precipitate pores. After subsequent washing, filtration, and vacuum drying for 48 h at 120°C, the silica-containing precipitate was impregnated with $KHCO_3$ in the usual manner and was finally re-dried in a vacuum oven for 16 h at 120°C.

The method used to prepare the alumina-containing precipitated iron catalysts employed an Fe/Cu precipitate of the desired composition that had already been vacuum dried. Under an atmosphere of dry nitrogen (to prevent exposure to atmospheric water), an appropriate amount of liquid aluminum sec-butoxide was dissolved in a volume of 2-butanol needed to just fill the pores of the precipitate sample and achieve "incipient wetness" (40 ml per 100 g of a typical dried 100Fe/5Cu precipitate). The required amount of dried Fe/Cu precipitate was added to the butoxide solution, and the resulting slurry was stirred for 16 h to ensure complete pore filling by the viscous alkoxide solution. Excess alcohol solvent was then removed by heating the mixture in a vacuum oven for 6 h at 60°C. Hydrolytic decomposition of the impregnated aluminum sec-butoxide to form $Al_2O_3$ was accomplished by exposure of the material for 16 h at 25°C to air that was saturated with water vapor. The alumina-containing catalysts, after being thoroughly washed and dried in a vacuum oven for 16 h at 120°C, were impregnated with $KHCO_3$ and were re-dried to yield the final catalysts.

## Elemental Analyses and Physical Properties

A total of 24 unsupported precipitated iron catalysts of differing compositions were synthesized (including pure, unpromoted iron), in which copper and potassium promoters were varied in the ranges 0.1 to 20 and 0.01 to 2.0 parts/100 parts of iron (by weight), respectively. In addition, three $SiO_2$-supported and three $Al_2O_3$- supported catalysts, each containing both copper and potassium promoters, were also prepared. The elemental composition of each prepared material was determined by atomic absorption spectroscopy; Table VII-1 summarizes the intended nominal and actual analyzed composition of each catalyst. For purposes of simplicity, each catalyst will be referred to in this document by its nominal composition.

Total surface areas, as measured by application of the BET method to $N_2$ adsorption at -196°C, were obtained for selected catalysts before and after reduction in $H_2$ or CO, and are presented in Table VII-2. Although total surface areas of the unsupported catalysts were relatively large (~ 180 $m^2/g$) prior to reduction and increased with increasing copper content

Table VII-1 Compositions of Synthesized Precipitated Iron Catalysts

| Nominal Composition (parts by weight) | Analyzed Composition (parts by weight) |
|---|---|
| 100Fe/0.01K | 100Fe/0.005K±0.001 |
| 100Fe/0.02K | 100Fe/0.016K±0.001 |
| 100Fe/0.05K | 100Fe/0.037K±0.004 |
| 100Fe/0.1K | 100Fe/0.082K±0.005 |
| 100Fe/0.2K | 100Fe/0.19K±0.01 |
| 100Fe/0.5K | 100Fe/1.01K±0.02 |
| 100Fe/1K | 100Fe/0.83K±0.06 |
| 100Fe/2K | 100Fe/1.7K±0.3 |
| 100Fe/0.1Cu | 100Fe/0.12Cu±0.01 |
| 100Fe/0.3Cu | 100Fe/0.29Cu±0.01 |
| 100Fe/0.3Cu/0.05K | 100Fe/0.27Cu±0.01/0.040K±0.002 |
| 100Fe/0.3Cu/0.2K | 100Fe/0.28Cu±0.01/0.185K±0.002 |
| 100Fe/0.3Cu/0.5K | 100Fe/0.28Cu±0.01/0.48K±0.07 |
| 100Fe/1Cu | 100Fe/1.04Cu±0.06 |
| 100Fe/1Cu/0.05K | 100Fe/0.94Cu±0.04/0.049K±0.004 |
| 100Fe/1Cu/0.2K | 100Fe/0.96Cu±0.03/0.18K±0.01 |
| 100Fe/1Cu/0.5K | 100Fe/1.05Cu±0.03/0.83K±0.04 |
| 100Fe/3Cu | 100Fe/2.97Cu±0.06 |
| 100Fe/3Cu/0.05K | 100Fe/2.83Cu±0.11/0.045K±0.001 |
| 100Fe/3Cu/0.2K | 100Fe/2.93Cu±0.12/0.18K±0.01 |
| 100Fe/3Cu/0.5K | 100Fe/2.95Cu±0.04/0.45K±0.03 |
| 100Fe/10Cu | 100Fe/9.7Cu±0.3 |
| 100Fe/20Cu | 100Fe/18.7Cu±0.4 |
| 100Fe/5Cu/4.2K/8$SiO_2$ | 100Fe/5.1Cu/4.0K/7.8$SiO_2$ |
| 100Fe/5Cu/4.2K/25$SiO_2$ | 100Fe/5.4Cu/4.6K/28$SiO_2$ |
| 100Fe/5Cu/4.2K/100$SiO_2$ | 100Fe/5.3Cu/4.1K/96.5$SiO_2$ |
| 100Fe/5Cu/4.2K/8$Al_2O_3$ | 100Fe/5.0Cu/3.9K/7.7$Al_2O_3$ |
| 100Fe/5Cu/4.2K/25$Al_2O_3$ | 100Fe/5.1Cu/4.0K/20.5$Al_2O_3$ |
| 100Fe/5Cu/4.2K/100$Al_2O_3$ | 100Fe/4.7Cu/4.2K/31.6$al_2O_3$ |

(to > 300 $m^2/g$ ) for 100Fe/3Cu, reduction in $H_2$ at 300°C for 4 h caused a decrease in surface area to ~ 10 $m^2/g$ in all cases. By contrast, the presence of even small amounts of $SiO_2$ support resulted in the retention of relatively high surface areas, even after reduction.

The pore size distribution of the unpromoted, unreduced iron precipitate gave an average pore diameter of 40-45 Å, as determined by application of the Kelvin equation to the desorption branch of a $N_2$ adsorption isotherm obtained at -196°C. The technique of mercury porosimetry was also employed to obtain the pore size distributions of calcined and reduced catalysts. Calcination for 16 h in air at 300°C caused an increase in the average pore diameter from the initial value of 40-45Å to 90Å. Subsequent reduction in $H_2$ at 300°C led to a bimodal pore size distribution, with the principal maximum at 250Å pore diameter for the unpromoted precipitate, and at 400Å for the copper-promoted precipitates containing 0.1 and 0.3 parts copper, with a secondary maximum at 90Å. The distribution of the pore volume for each of the three silica- containing catalysts following calcination for 5 h at 300°C and reduction in CO for 5 h at 300°C differed, depending upon $SiO_2$ content. The $8SiO_2$ material exhibited a well-defined maximum at a pore diameter of 150-200Å , while the $25SiO_2$ and the $100SiO_2$ precipitates contained a substantial fraction of pores smaller than 60Å after reduction in CO.

### VII.2. Reduction Studies

Temperature-programmed (TPR) and isothermal reduction studies were performed using both 5% $H_2/N_2$ and 5% CO/He as reductants. The reactive gas streams were first directed at a constant rate and at a constant pressure through the reference compartment of a thermal conductivity (TC) cell via a two-way injection valve, through the catalyst sample, and finally, via a cold trap, through the other compartment of the TC detection cell. Consumption of CO or $H_2$ was measured by the change in thermal conductivity of the effluent gas stream. In addition, the reactor effluent was monitored by a quadrupole mass spectrometer to provide continuous chemical identification of reduction/desorption products. A dry ice/acetone bath was used to remove water formed during the hydrogen reductions, and a liquid nitrogen bath was used to remove $CO_2$ formed during the CO reductions. Catalyst sample weights of 10 to 15 mgms and reductant flow rates of 12 cc/min were used for all the experiments. A temperature ramp of 20°C/min from room temperature to 900°C was used for all of the temperature-programmed reduction experiments. In isothermal reductions, a ramp of 20°C/min was used until a temperature of 300°C was reached, the latter temperature then being maintained until total heating times of 12 h for hydrogen reduction or 8 h for CO reduction were achieved. The

Table VII-2 Surface Areas of Synthesized Precipitated Iron Catalysts

| Nominal Composition (parts by weight) | Surface Area ($m^2/g$) | |
|---|---|---|
| | Unreduced | Reduced |
| 100Fe | 180 | 10 * |
| 100Fe/0.01K | 195 | - |
| 100Fe/0.02K | 205 | - |
| 100Fe/1K | 210 | - |
| 100Fe/0.1Cu | 280 | 5 * |
| 100Fe/0.3Cu | 328 | 5 * |
| 100Fe/0.3Cu/0.5K | 285 | - |
| 100Fe/1Cu | 234 | - |
| 100Fe/1Cu/0.05K | - | 8 * |
| 100Fe/1Cu/0.5K | 231 | 9 * |
| 100Fe/3Cu | 300 | 5 * 38 ** |
| 100Fe/10Cu | 380 | - |
| 100Fe/20Cu | 374 | 8 * |
| 100Fe/5Cu/4.2K/8$SiO_2$ | | 94 ** |
| 100Fe/5Cu/4.2K/25$SiO_2$ | | 150 ** |
| 100Fe/5Cu/4.2K/100$SiO_2$ | | 250 ** |

* In flowing $H_2$ for 4 hrs at 300°C

** In flowing CO for 4 hrs at 300°C

reduction of a CuO wire was used for calibration of the peak areas in reduction results.

Typical TPR results using $H_2$ reductant are shown in Figure VII-2 for a series of copper-promoted iron precipitates containing no potassium. The two peaks in the lowermost thermogram for the unpromoted copper-free sample correspond to the following characteristic two-step reduction of $Fe_2O_3$ that was observed for most of the catalysts studied:

$$3Fe_2O_3 + H_2 \rightarrow 2Fe_3O_4 + H_2O \qquad (VII-1)$$

$$Fe_3O_4 + 4H_2 \rightarrow 3Fe + 4H_2O \qquad (VII-2)$$

Because reaction (VII-2) consumes eight times as much $H_2$ per mole of Fe as does reaction (VII-1), it is clear from the relatively small area of the second peak in this thermogram that only a small fraction of the iron in the sample is converted to the metallic state by this treatment in $H_2$. Comparison of the thermograms in Figure VII-2 demonstrates that increasing concentrations of copper promoter, up to a level of 3 wt%, decrease the temperatures required for the onset of both reduction steps. Copper contents greater than 3 wt% had little additional promotional effect on iron reduction. The presence of varying concentrations of potassium promoter, in the absence of copper, had little effect on iron thermograms in $H_2$, as shown by the data in Figure VII-3.

In order to more closely mimic the reduction procedure used during actual catalyst activation, a modified version of the TPR technique was employed, in which the sample temperature was ramped at 20°C/min to 300°C, and then maintained isothermally at the latter temperature in the flowing reductant stream. Typical results obtained from this "isothermal" reduction process, using $H_2$ reductant, are shown in Figure VII-4 for selected copper-promoted samples. Although the first reduction step occurs rapidly in all cases, as shown by the sharp peak at 50 min, it is again evident that the presence of even small concentrations of copper promoter greatly decreases the time required for completion of the second reduction step. Whereas more than 900 min were required to complete reduction of the unpromoted sample (a), reduction was complete in 400 min in the presence of 3 wt% of copper (d). The presence of potassium promoter, in the absence of copper, actually decreased the rate of the first reduction step, as shown in Figure VII-5 by the increased broadening of the first peak with increasing potassium content. This effect was probably due to nucleation site blockage by potassium which, because

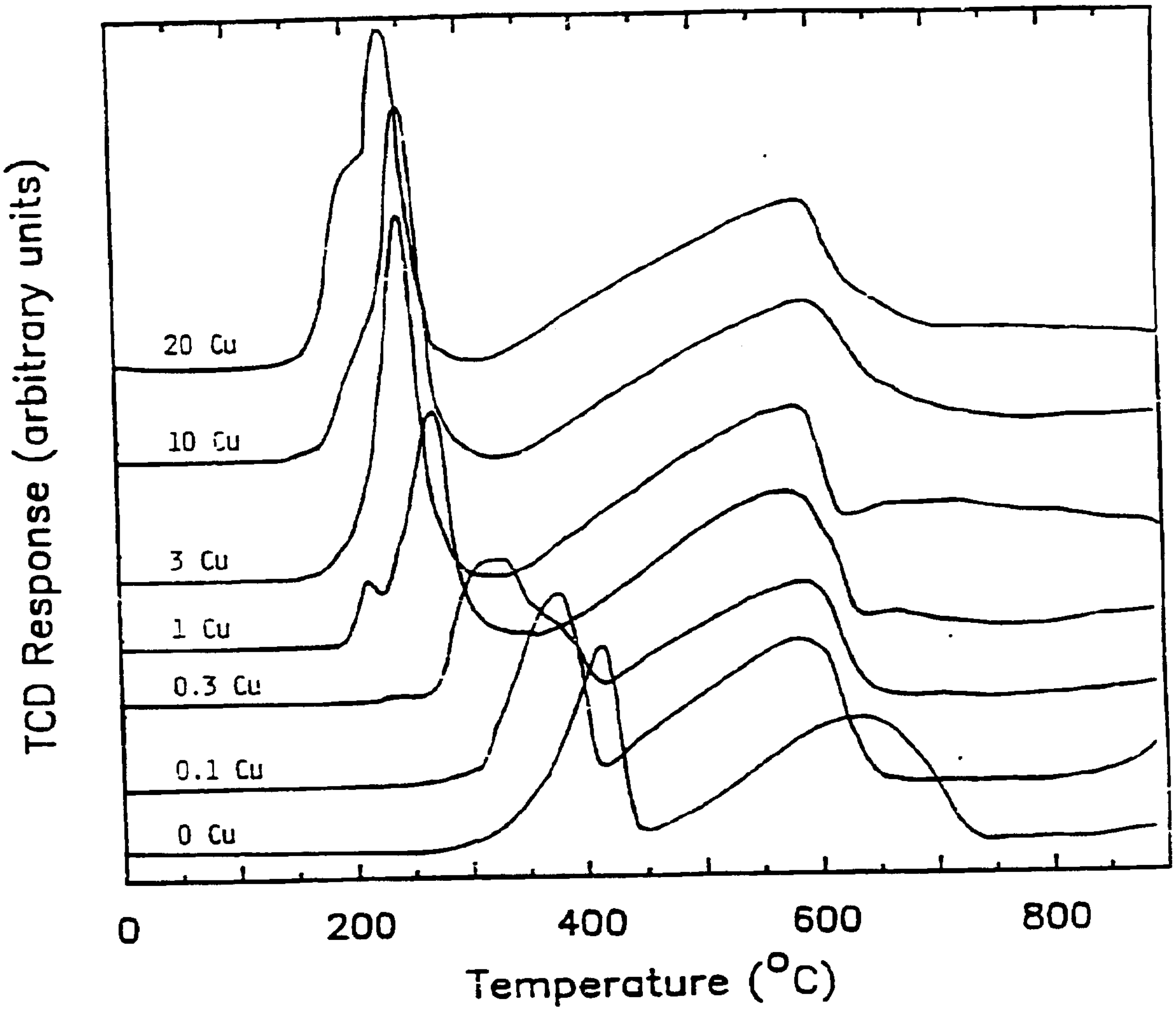

Figure VII-2 TPR profiles of potassium-free, pre-calcined iron catalysts containing the indicated levels of copper promoter (in parts by weight per 100 parts of Fe)

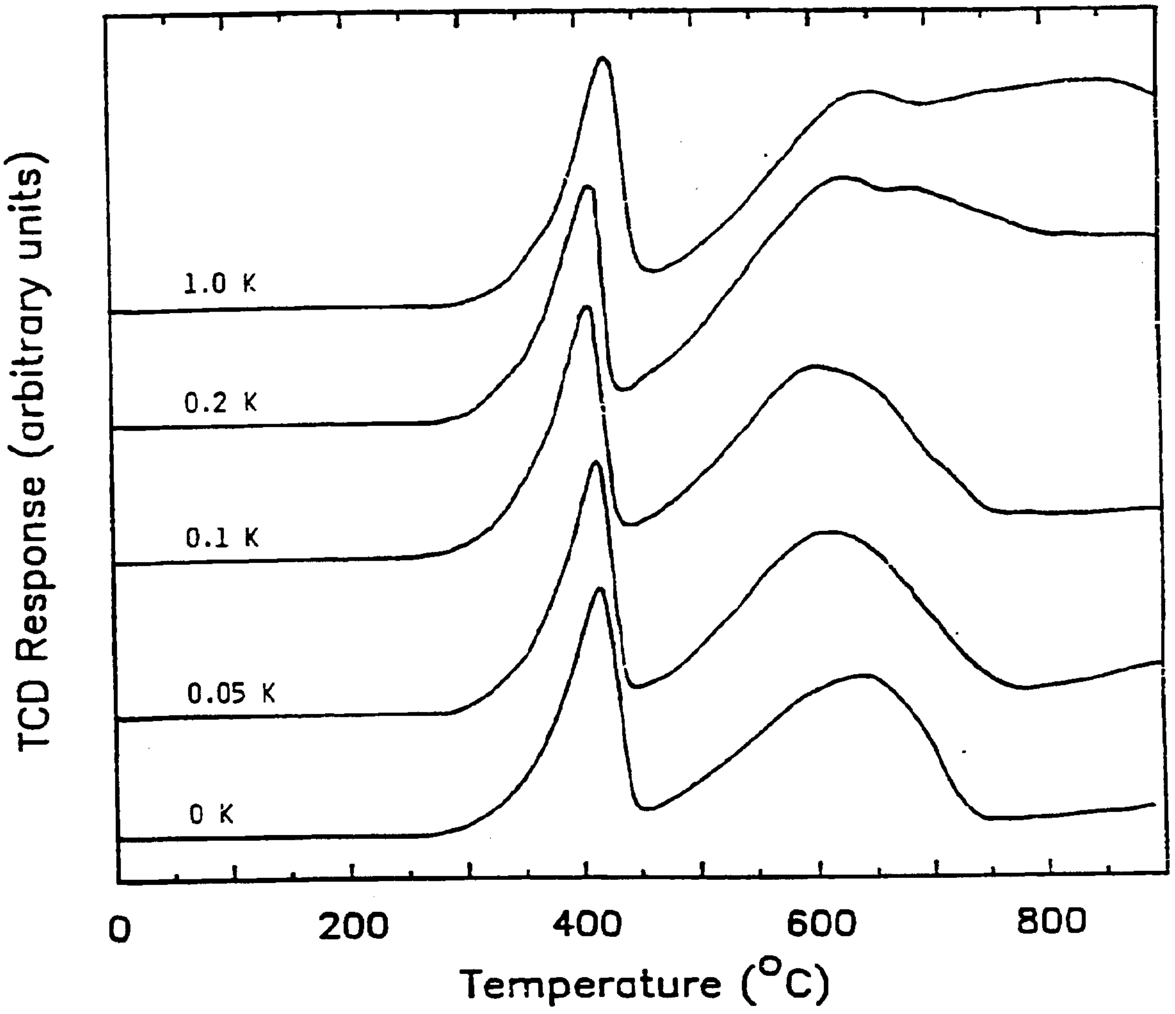

Figure VII-3 TPR profiles of copper-free, pre-calcined iron catalysts containing the indicated levels of potassium promoter (in parts by weight per 100 part of Fe)

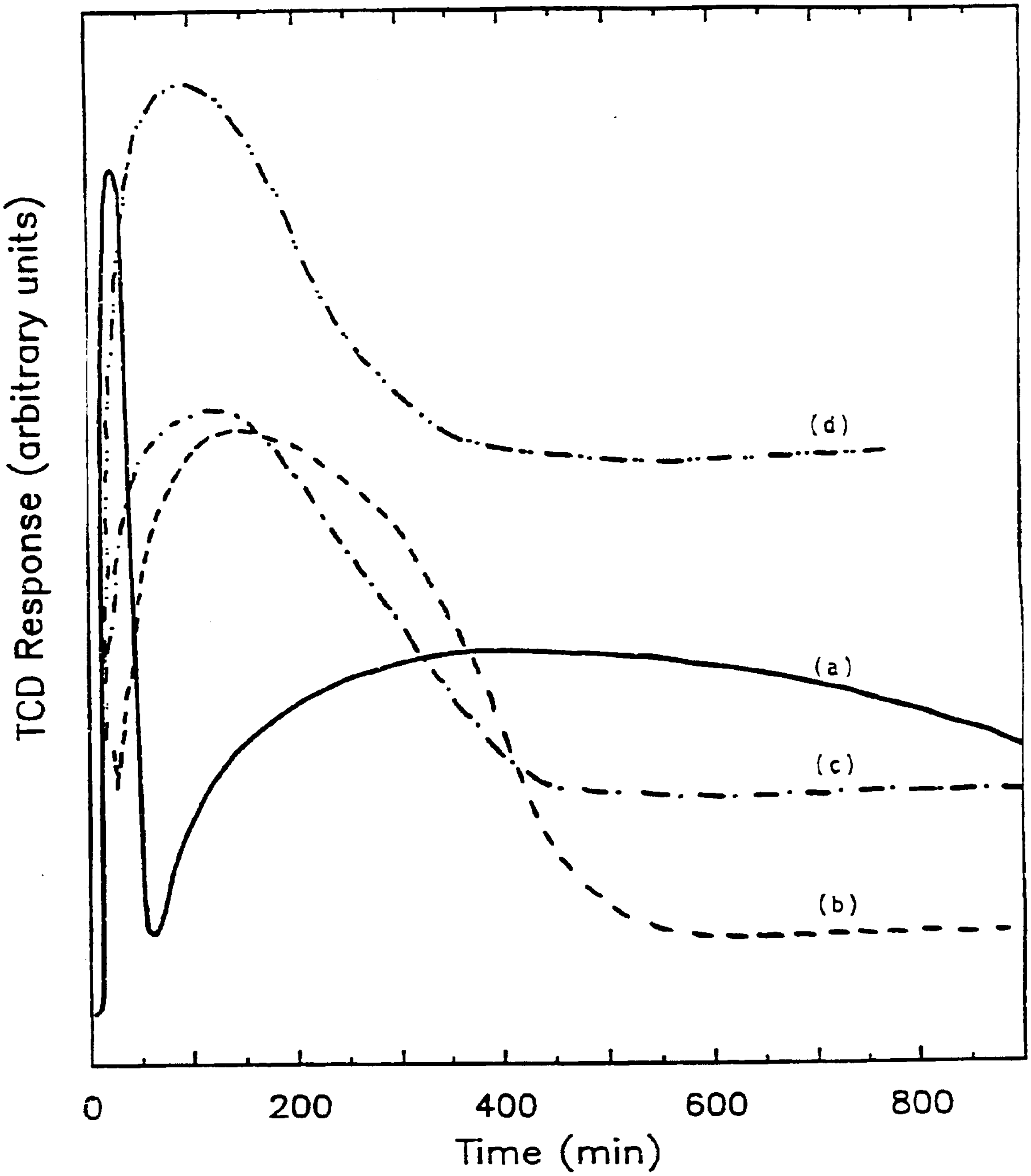

Figure VII-4 Isothermal reduction profiles in $H_2$ at 300°C of: (a) 100Fe; (b) 100Fe/0.3Cu; (c) 100Fe/1.0Cu; (d) 100Fe/3.0Cu of the presence of water vapor generated during $H_2$ reduction of iron, had redistributed into a thin surface layer.

Carbon monoxide proved to be a much more effective reducing agent for precipitated iron than was $H_2$, as demonstrated by the results shown in Figure VII-6. (Note the different abscissa scale from that in Figures VII-4 and VII-5.) The second reduction step, that required > 900 min to complete for the unpromoted sample when treated in $H_2$, was complete in 240 min using CO as the reducing agent (a). The presence of 1 wt% copper promoter further decreased the time required for complete reduction to 100 min (d). In marked contrast to the reduction behavior observed using $H_2$, potassium promoter, in the absence of copper, appeared to increase the rate of iron reduction, as shown in thermograms (b) and (c). Moreover, the addition of potassium to a copper- containing catalyst resulted in more rapid reduction than that observed in the presence of copper alone (e).

## VII.3. Surface Characterization

X-ray photoelectron spectroscopy (XPS) measurements were used to study the surface compositions and oxidation states of the precipitated iron catalysts before and after calcination and reduction treatments. Samples used in the XPS measurements were pressed into thin wafers to fit the copper sample holder and the sample probe of the spectrometer. After either reduction or reaction, samples were evacuated for one hour and were transferred, without exposure to the air, to the antechamber of the glove box attached to the spectrometer. The antechamber was evacuated and back-filled with nitrogen before the sample was admitted to the glove box. An aluminum sample cover with a rectangular opening, plated with a 50 nm thickness of gold by a high-voltage evaporation method, was placed on top of the sample. A stainless steel spring placed under the sample holder ensured electrical contact of the sample with the instrument. Typical analysis chamber pressure during measurements was $< 1 \times 10^{-9}$ torr. The beam power of the X-ray was 600 watts, and a flood gun, set at 0.1 mA and 0 eV, was used to eliminate sample charging. Adventitious carbon and the support oxygen species were used as references. Various scan numbers and binding energies were obtained for the major peaks of the elements of interest, depending on the amount present and the cross-section.

The type of information obtainable by XPS measurements is illustrated in Figure VII-7, which shows spectra in the Fe 2p region for an unpromoted iron sample before and after reduction in $H_2$. It is clear that treatment in $H_2$ at 300°C results in only a small fraction of zero-valent surface iron. Treatment in CO at 300°C, on the other hand, effects almost

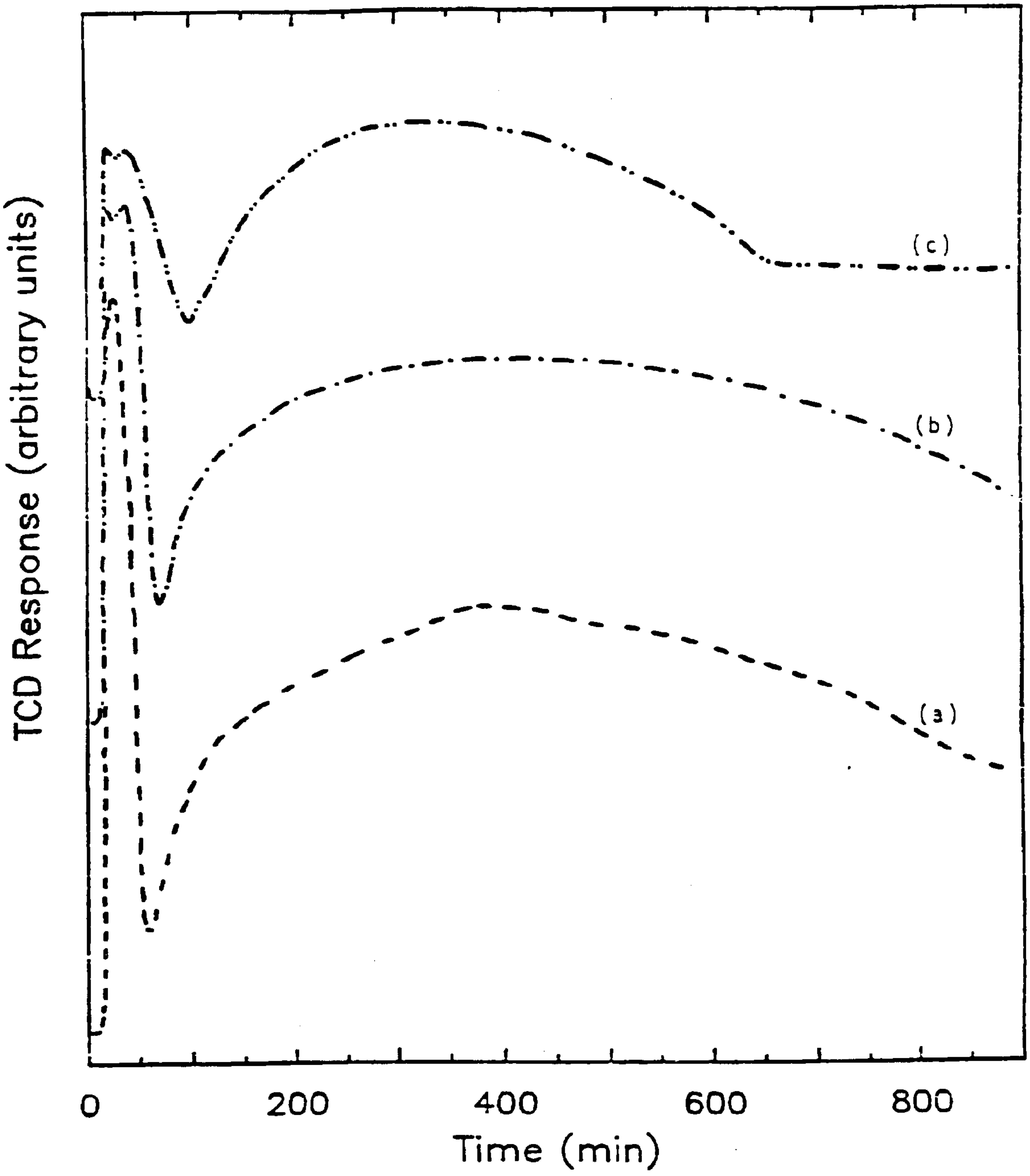

Figure VII-5 **Isothermal reduction profiles in $H_2$ at 300°C of: (a) 100Fe/0.2K; (b) 100Fe/1.0K; 100Fe/2.0K**

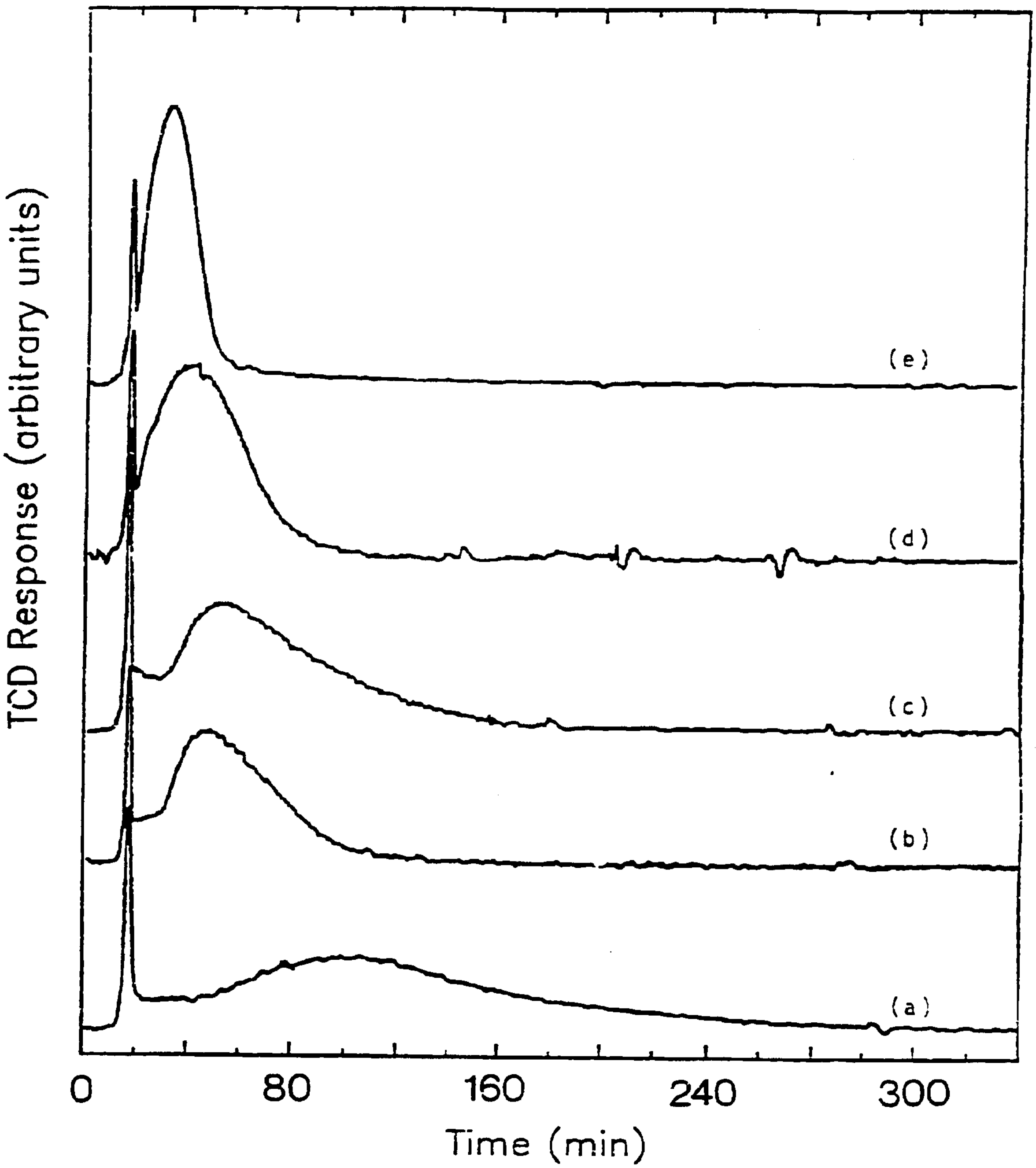

Figure VII-6 Isothermal reduction profiles in CO at 300°C of: (a) 100Fe; (b) 100Fe/0Cu/0.2K; (c) 100Fe/0Cu/1.0K; (d) 100Fe/1.0Cu/0K; (e) 100Fe/1.0Cu/0.2K complete surface reduction to the metallic state, as shown in Figure VII-8. It is also apparent from spectrum (b) in the latter Figure that subsequent exposure of the reduced catalyst to a 2/1 $H_2$/CO reaction mixture at 250°C results in re-oxidation of a portion of the surface iron by water formed during CO hydrogenation.

As expected, the presence of copper promoter increased the extent of surface iron reduction to the metallic state, even with supported catalysts, as shown by spectrum (a) in Figure VII-9 for the $100Fe/5Cu/4.2K/8SiO_2$ composition. Subsequent exposure to a $H_2$/CO reaction mixture again caused partial re-oxidation of surface iron (spectrum b). Although treatment of the promoted catalyst in CO did not result in more extensive surface reduction than that observed following $H_2$ treatment, the CO-treated material underwent much less subsequent oxidation during $H_2$/CO reaction, as shown in Figure VII-10. Reduction in CO caused extensive deposition of surface carbon (Figure VII-11), which was removed, presumably by hydrogenation, during exposure of the reduced catalyst to a $H_2$/CO reaction mixture at 250°C.

## VII.4. Summary of Results and Discussion

The results obtained during this investigation have demonstrated that reduction studies under either isothermal conditions or a constant temperature-programming rate can differentiate reducibilities of bulk compositions, but not of surface compositions of iron catalysts. Figures VII-12 and VII-13 summarize the temperature locations of the peak corresponding to the first step of iron reduction in TPR profiles for the copper-, potassium-, and silica-containing catalysts. Isothermal reduction results are summarized in Table VII-3, which shows approximate times required for completion of the second step of iron reduction to Fe(0). XPS studies, whose results are summarized in Table VII-4, have complemented these reduction studies by providing information about the identities of the surface iron phases.

### VII.4.1. Reduction Behavior of Precipitated Iron Catalysts

TPR results obtained for precipitated iron catalysts are dependent on both the amounts and identities of promoters and on pretreatment. Figure VII-12 summarizes the peak locations ($T_m$) of the first step of iron reduction for the precalcined copper-promoted catalysts, and illustrates the decrease in $T_m$ with increasing copper content. $T_m$'s for the second step of iron reduction of precipitated iron catalysts do not change appreciably with copper content, but the temperature at which the second step commences decreases. The more facile reduction of copper oxide could be attributed to the relatively lower molar free energy of reduction for the copper oxide (-100 kJ/mole at 25°C) compared to that for the corresponding iron compound

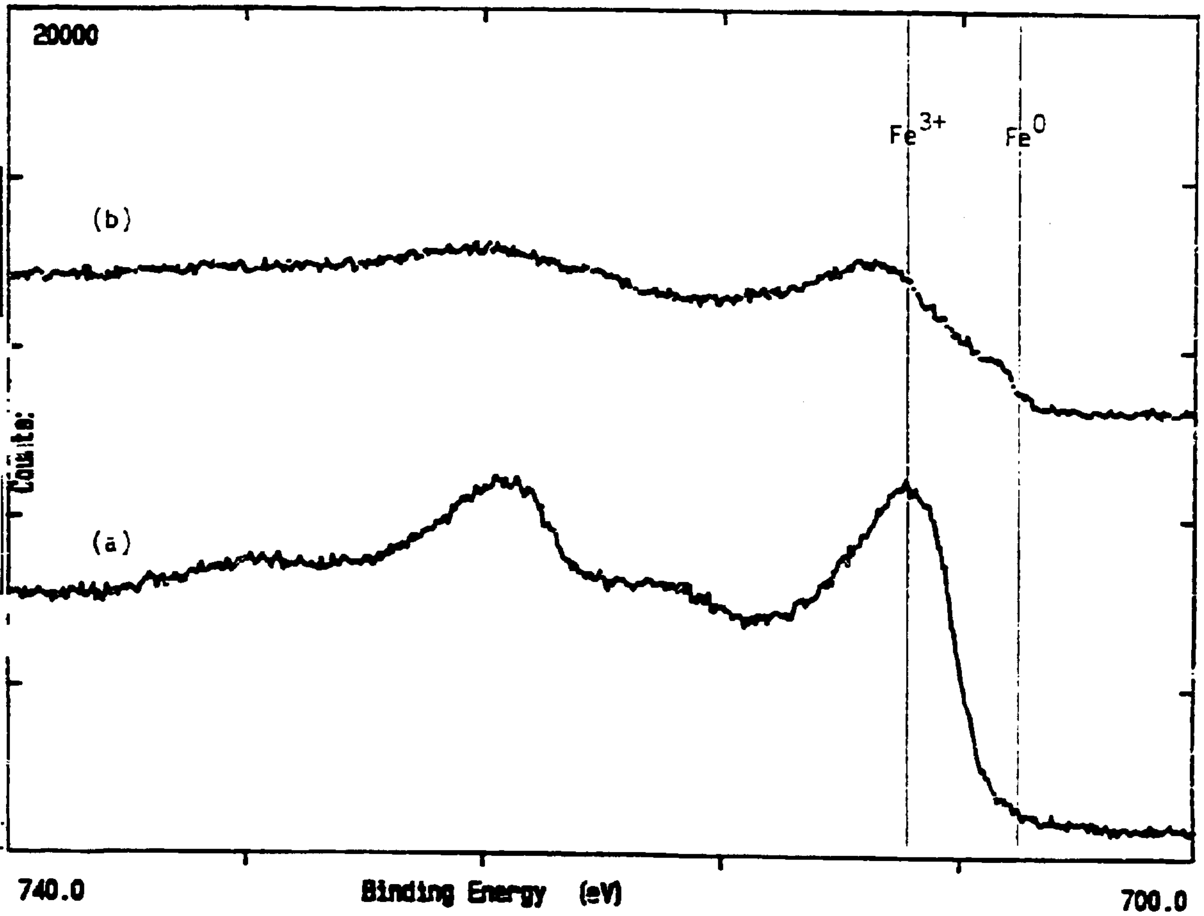

Figure VII-7 XPS spectra of unpromoted 100Fe precipitate in Fe 2p region: (a) following calcination for 5 hrs at 300°C; (b) following subsequent exposure to $H_2$ for 5 hrs at 300°C

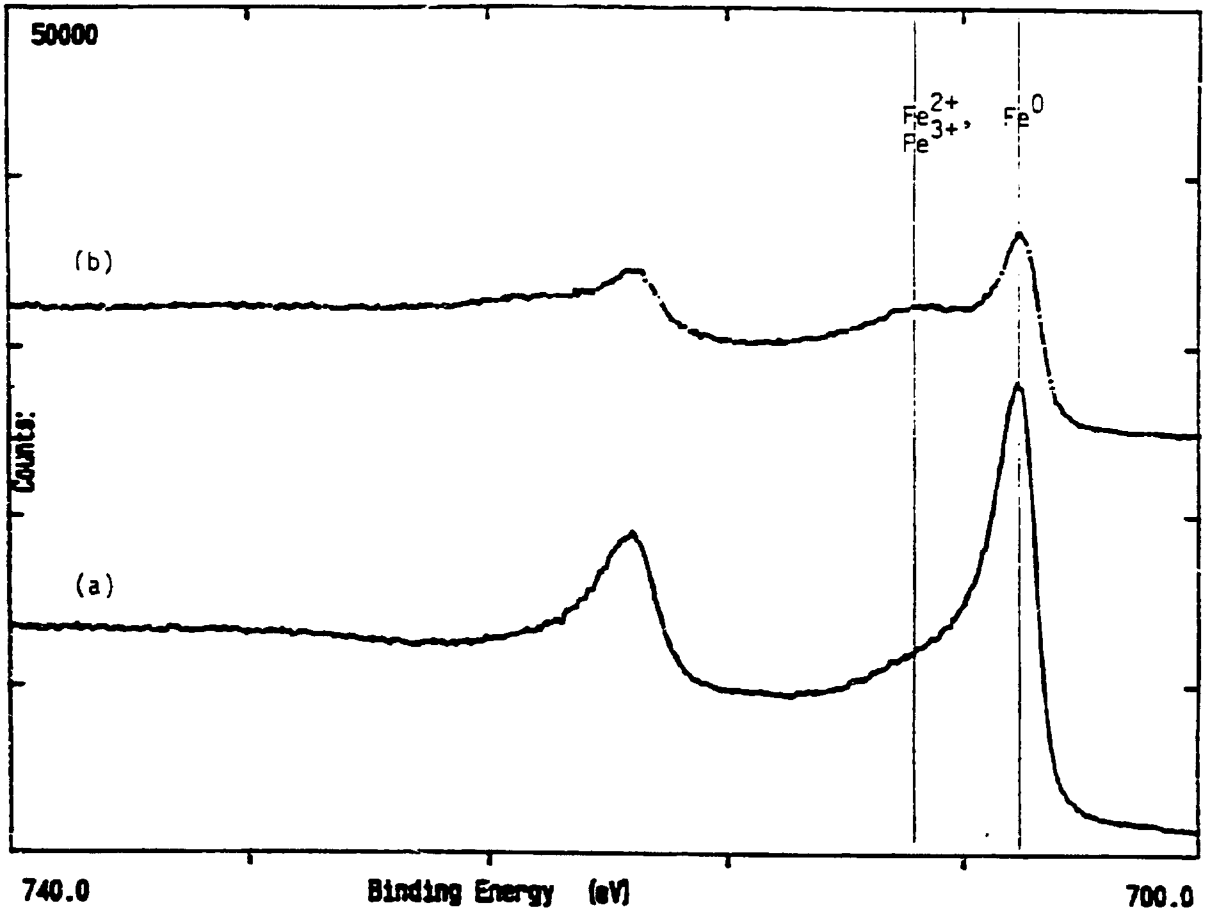

Figure VII-8 XPS spectra of unpromoted 100Fe precipitate in Fe 2p region: (a) following calcination for 5 hrs at 300°C and subsequent reduction in CO for 5 hrs at 300°C; (b) following subsequent exposure to 2/1 mixture of $H_2$/CO at 250°C and 1 atm

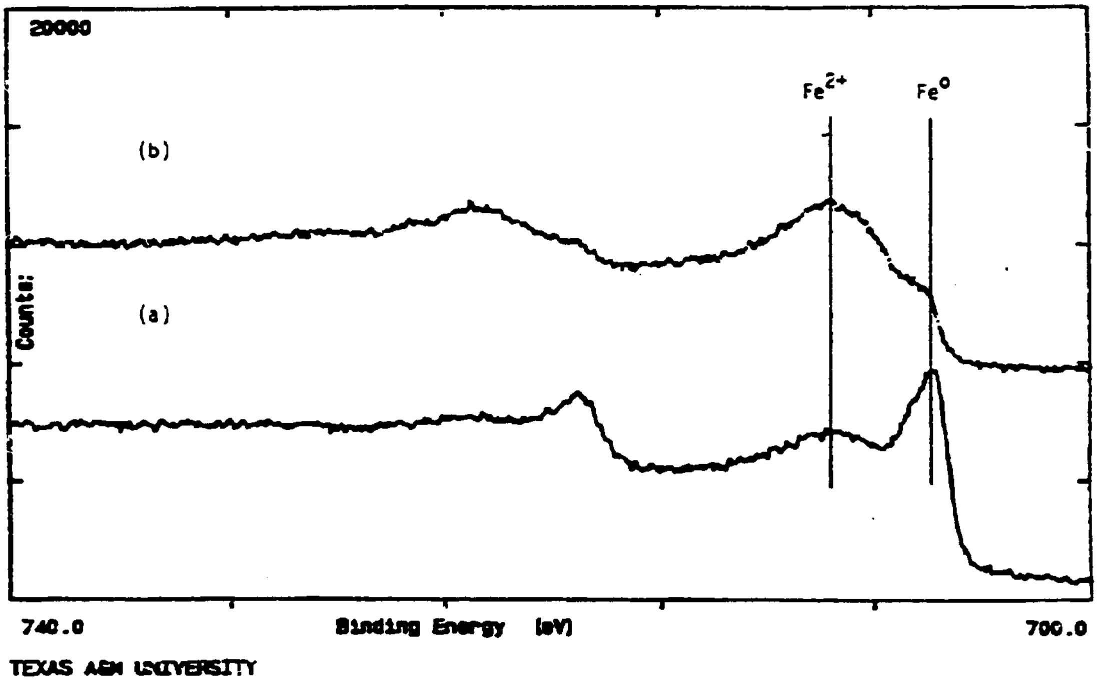

Figure VII-9 XPS spectra of 100Fe/5Cu/4.2K/8SiO$_2$ in Fe 2p region: (a) following exposure to H$_2$ at 300°C; (b) following subsequent exposure to H$_2$/CO at 250°C

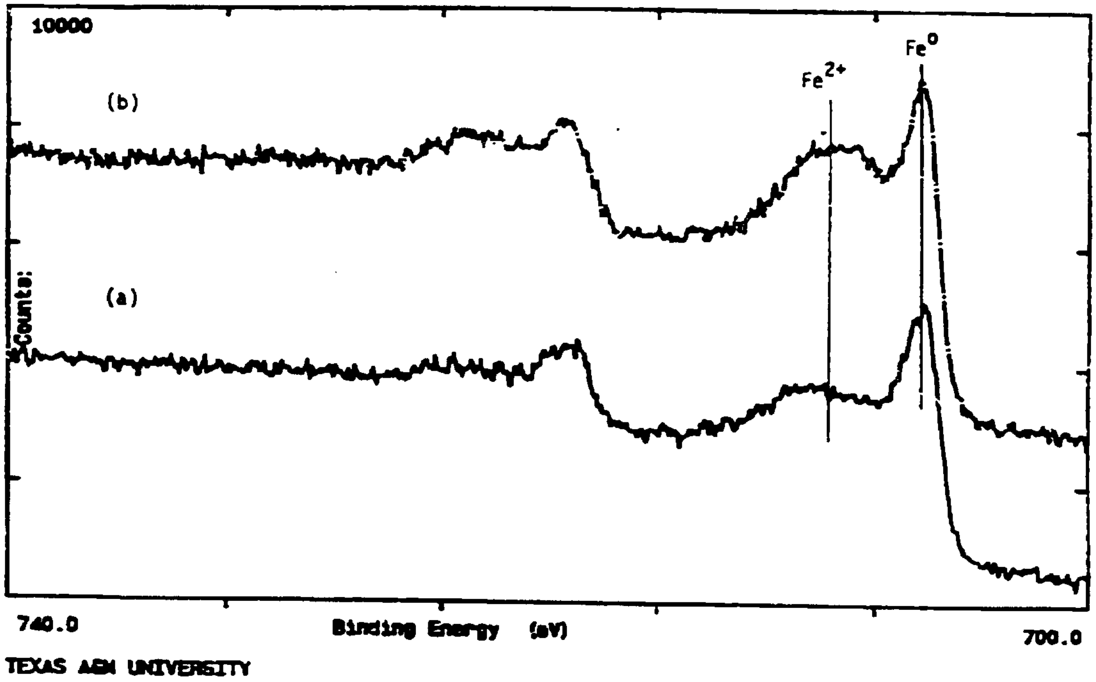

Figure VII-10 XPS spectra of 100Fe/5Cu/4.2K/8SiO$_2$ in Fe 2p region: (a) following exposure to CO at 300°C; (b) following subsequent exposure to H$_2$/CO at 250°C

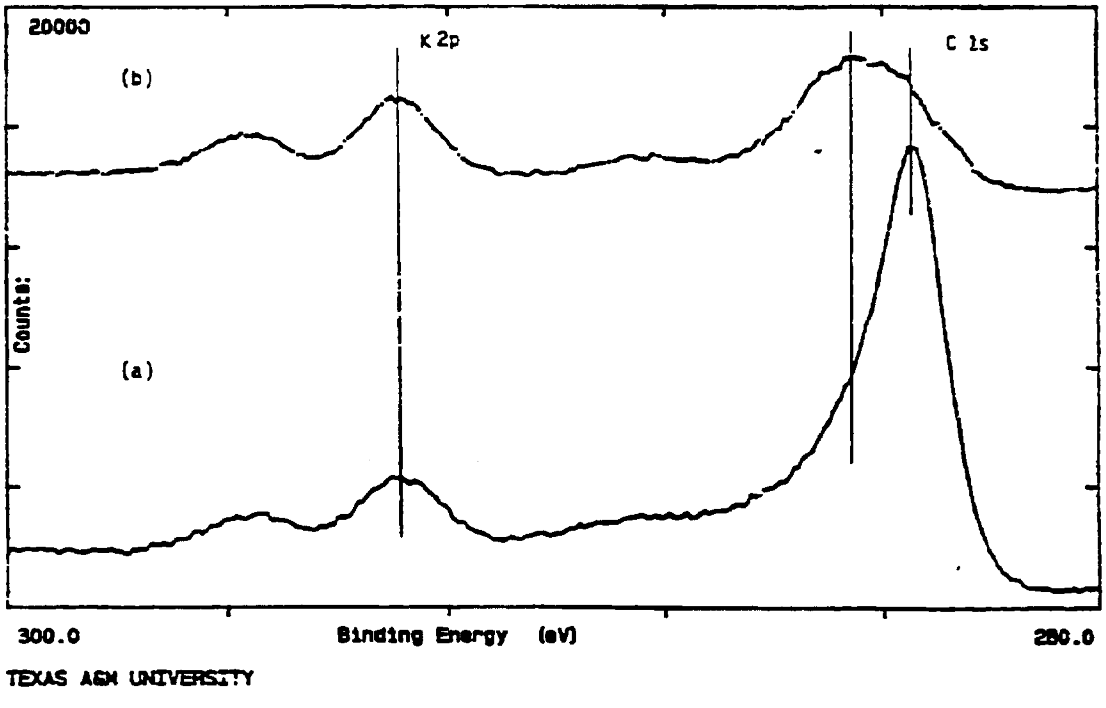

Figure VII-11 XPS spectra of 100Fe/5Cu/4.2K/8SiO$_2$ in K 2p and C 1s regions: (a) following exposure to CO at 300°C; (b) following subsequent exposure to H$_2$/CO at 250°C

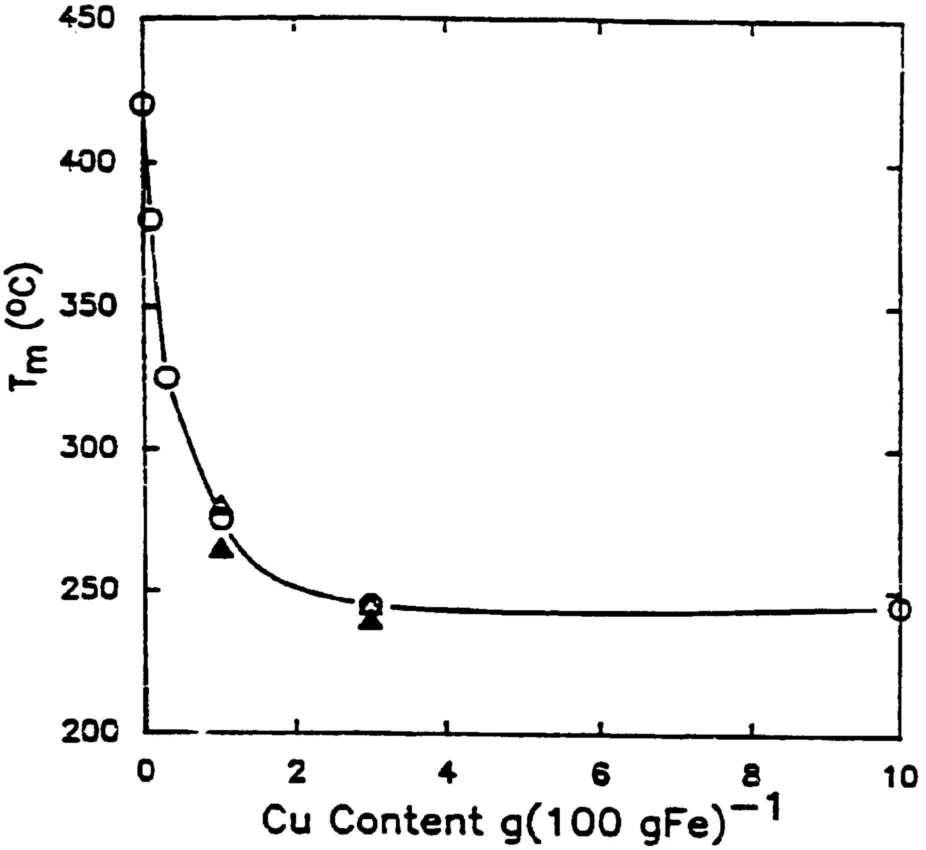

Figure VII-12 **Influence of copper promoter on TPR peak maximum for the first step of iron reduction: open circle, potassium-free catalysts; filled triangle, catalysts containing 0.05 part potassium; open triangle, catalysts containing 0.2 part potassium**

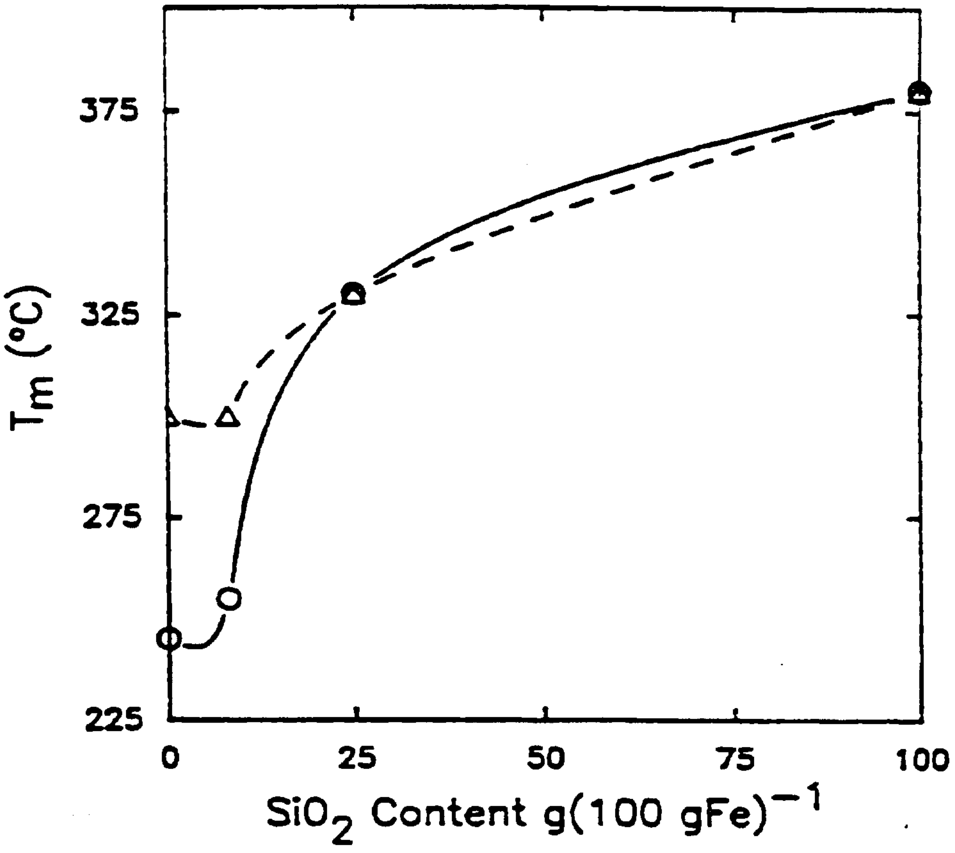

Figure VII-13 Influence of $SiO_2$ support on TPR peak maximum for the first step of iron reduction: open circle, catalysts containing 5 parts copper; open triangle, catalysts containing 5 parts copper and 4.2 parts potassium

(20 kJ/mole at 25°C) (Jones and McNicol, 1986). According to the nucleation mechanism of oxide reduction, the reduction of oxide accelerates as the first metal nuclei are formed (Madon and Taylor, 1981). The lower reduction temperature required for copper oxide relative to iron oxide leads to formation of nucleation sites in metallic copper at temperatures where metallic iron would not normally be formed; an increase in the number of nucleation sites accelerates the subsequent reduction of iron oxide. It is evident from Table VII-3 that the time required for the completion of iron reduction in either $H_2$ or CO decreases with increasing copper content.

Copper-promoted iron catalysts were prepared by the co-precipitation of copper nitrate solution with iron nitrate solution, resulting in a uniform distribution of copper throughout the catalysts. Even at very low levels (0.1 wt%), copper exerts a significant effect as a structural promoter to prevent precipitated iron oxide from forming large particles, resulting in an increase in total surface area (Table VII-2). Catalyst surface areas decrease considerably, however, after calcination, both with and without copper promoters. The TPR profiles before and after calcination illustrate the dependence of the bulk composition on catalyst pretreatment. In addition, removal of water and nitrate by pre-calcination also cause a composition change in the surface phase which can be observed from XPS results. Since the basic two-stage iron reduction feature in TPR profiles for the copper-promoted iron catalysts is similar to that observed for the unpromoted iron catalyst, it is unlikely that true alloying between iron and copper occurred. This observation is in agreement with previous results, which indicate that alloying between copper and iron becomes significant only at temperatures above 700°C (Hansen, 1958). The presence of potassium causes a change in the TPR profiles for the copper-promoted catalysts, suggesting that the potassium is capable of influencing the reduction of copper.

Unlike copper oxide, potassium oxide cannot be reduced in either $H_2$ or CO (at the temperatures employed in this study), compared to the reduction temperature of iron, to form nucleation sites. The temperature locations of the first step of iron reduction in the TPR results do not change with potassium content, as shown in Figure VII-3. In the absence of copper, the time required for completion of the first step of iron reduction in $H_2$ increases with increasing potassium content, suggesting that a blockage of nucleation sites by potassium may inhibit the reduction of iron. However, a different effect is observed in the treatment of catalysts using CO. Table VII-3 indicates that the time required for the completion of iron reduction in CO decreases in the presence of potassium. This promotional effect may be attributed to the facilitation of CO dissociation in the presence of potassium on the surface of iron.

Table VII-3 Time Required for Completion of Second Step of Iron Reduction at 300°C

| Catalyst (parts by weight) | Time (min) in $H_2$ | Time (min) in CO |
|---|---|---|
| 100Fe | >1000 | 360 |
| 100Fe/0.2K | >1000 | 120 |
| 100Fe/1K | >1000 | 180 |
| 100Fe/0.3Cu | 600 | 120 |
| 100Fe/1Cu | 480 | - |
| 100Fe/3Cu | 400 | 80 |
| 100Fe/1Cu/0.05K | 560 | 60 |
| 100Fe/1Cu/0.2K | 560 | 60 |
| 100Fe/3Cu/0.2K | 300 | 60 |

The reduction results in Figure VII-13 show that the reduction of iron is inhibited by the addition of a support, suggesting an interaction between metal and support, which has been proposed by many investigators (Dry, 1981; Anderson, 1984; Lund and Dumesic, 1981). The promotional effect of copper is gradually eliminated by increasing contents of both silica and alumina, due to the interaction between metal and support. The addition of potassium magnifies the inhibition effect of support on the reduction of copper and iron because the presence of potassium suppresses the promotional effect of copper on the reduction, due to the covering of nucleation sites by potassium. The transport of $SiO_2$ on iron oxide in $H_2O$-containing environments has been proposed by Lund and Dumesic (1981). They measured the movement of $SiO_2$ over the surface of an oxidized iron foil at 400°C and atmospheric pressure in different gas environments by scanning Auger electron microscopy. Silica migration was observed upon treatment in $H_2O/CO$ or $H_2O/H_2$ gas mixtures, while significant migration was not observed upon treatment in $CO_2/CO$ or $O_2$. In the current investigation, the calcination/drying procedure may cause this type of support migration.

### VII.4.2. The Oxidation States of Surface Iron

The XPS results summarized in Table VII-4 indicate that the surfaces of the $H_2$-treated iron samples are largely covered by a layer of iron oxide. Although the isothermal reduction results for the $H_2$-reduced catalysts indicate extensive reduction of iron to Fe(0), the absence of metallic iron on the catalyst surface after $H_2$ treatment can be explained by the re-oxidation of iron by water, a by-product of reduction in $H_2$. By contrast, the XPS results indicate that the surfaces of the CO- treated samples possess the same compositions as those of the bulk, viz., zero-valent iron. One of the reasons for the absence of oxidized iron phases can be attributed to the formation of $CO_2$, instead of $H_2O$ as in the $H_2$ reduction, as a by-product of reduction in CO.

For potassium-promoted iron catalysts, the K 2p regions in XPS spectra indicate that reduction in $H_2$ leads to a pronounced spreading of potassium on the surface, compared to CO treatment (Table VII-4). The addition of potassium to the iron catalysts in this study was performed by impregnation with $KHCO_3$ solution. After drying in a vacuum oven at 120°C, the potassium formed an oxidized compound, as indicated by the lack of an increase in the carbonate carbon peak at 289 eV compared to that for the potassium-free catalyst. Similar experiments have been performed on a potassium-promoted iron catalyst which was prepared by impregnating a passivated iron powder with $K_2CO_3$ (Dwyer and Hardenberg, 1984;

Table VII-4 **Summary of XPS results for Precipitated Iron Catalysts**

| Catalyst (parts by weight) | Reductant* | % Fe(0) | % $Fe^{n+}$ | K $2p_{3/2}$ : Fe $2p_{3/2}$ |
|---|---|---|---|---|
| 100Fe | $H_2$ | 5 | 95 | - |
| | CO | 100 | - | - |
| 100Fe/3Cu | $H_2$ | 7 | 93 | - |
| | CO | 95 | 5 | - |
| 100Fe/0.2K | $H_2$ | - | 100 | - |
| | CO | 90 | 10 | - |
| 100Fe/2K | $H_2$ | - | 100 | 0.9 |
| | CO | 100 | - | 0.3 |
| 100Fe/3Cu/0.2K | $H_2$ | 55 | 45 | 0.5 |
| | CO | 100 | - | - |
| 100Fe/5Cu/4.2K/8$SiO_2$ | $H_2$ | 45 | 55 | 1.2 |
| | CO | 60 | 40 | 0.2 |
| 100Fe/5Cu/4.2K/25$SiO_2$ | $H_2$ | 50 | 50 | <0.1 |
| | CO | 30 | 70 | <0.1 |
| 100Fe/5Cu/4.2K/8$Al_2O_3$ | $H_2$ | 55 | 45 | 0.9 |
| | CO | 50 | 50 | 0.2 |
| 100Fe/5Cu/4.2K/25$Al_2O_3$ | $H_2$ | 4 | 96 | 0.1 |
| | CO | 40 | 60 | 0.5 |

*for 12 hrs at 300°C

Dwyer, 1985). Using XPS spectra, these workers have shown that $K_2CO_3$ was present on the surface of the catalyst before hydrogen reduction. They proposed that a surface KOH layer was formed from the partial decomposition of $K_2CO_3$. The same conclusion was first reached by Bonzel and Krebs (1987) in investigating the effects of $K_2CO_3$ coverage of an iron foil on Fischer-Tropsch synthesis. Using XPS measurements in the K 2p region, they showed that the potassium, associated in some form with oxygen, appeared not to be covered by the deposited carbon but rather resided on top of the carbon layer. However, an increase in the intensity of the carbonate carbon peak after $H_2$ reduction in this study seems not to be associated with potassium, because no corresponding increase in this peak intensity is observed after CO treatment.

The appearance of potassium on the surfaces of catalysts is complicated by the presence of a support. As the silica content increased to 25 parts per 100 parts of iron, no significant surface enrichment in potassium is observed after $H_2$ reduction at 300°C, indicating that the homogeneously distributed silica matrix inhibits the potassium migration process. For alumina-supported iron catalysts, a complicated K 2p XPS peak feature indicates that potassium can be associated with iron and with alumina as well. Arakawa and Bell (1983) postulated that a significant proportion of the potassium was consumed by acidic sites on the alumina support, leaving little available for interaction with the iron. Therefore, unlike the silica-supported iron catalysts, the presence of 20 parts of alumina per 100 parts of iron still shows a significant surface migration of potassium.

## VII.5. Conclusions

In this study, precipitated iron catalysts were characterized using temperature-programmed reduction, isothermal reductions and X-ray photoelectron spectroscopy. The following conclusions may be drawn from the results on this investigation:

1. $H_2$ and CO treatments of precipitated iron catalysts result in different surface compositions of catalysts. Water, a by-product of $H_2$ reduction, is a principal factor determining the reducibility of catalysts and the effects of promoters.
2. The promotional effect of copper on the reduction of iron increases with increasing copper content, up to 3 wt%.
3. The presence of potassium influences the reducibility of the precipitated catalysts, with or without copper.
4. The inhibition effect of silica and alumina supports on the reduction of iron increases with

increasing support content. The inhibition effect is less pronounced for alumina than for silica.